

Received January 2, 2020, accepted January 14, 2020, date of publication January 17, 2020, date of current version January 27, 2020.

Digital Object Identifier 10.1109/ACCESS.2020.2967435

# Optimal Location and Capacity of the Distributed Energy Storage System in a Distribution Network

XIAOBO TANG<sup>1</sup>, KAI DENG<sup>1</sup>, QIUWEI WU<sup>1,2</sup>, (Senior Member, IEEE), AND YULONG FENG<sup>1</sup>

<sup>1</sup>School of Electrical and Automation Engineering, Nanjing Normal University, Nanjing 210023, China

<sup>2</sup>Center for Electric Power and Energy, Department of Electrical Engineering, Technical University of Denmark, 2800 Lyngby, Denmark

Corresponding author: Xiaobo Tang (61058@njnu.edu.cn)

This work was supported by the Postgraduate Research and Practice Innovation Program of Jiangsu Province under Grant KYCX19\_0801.

**ABSTRACT** Given the current situation of large-scale energy storage system (ESS) access in distribution network, a practical distributed ESS location and capacity optimization model is proposed. Firstly, a weighted voltage sensitivity is proposed to select the grid-connected node set of ESS. On this basis, the distributed ESS location model is established, which aims at reducing voltage deviation and active power loss of the distribution network. Then, an ESS partition method based on the improved flame propagation model is proposed, and the partition results are obtained by constructing the flammability of nodes, the wind direction of flame propagation, speed of flame propagation and other indicators. Based on partition results, the capacity optimization model is established with the maximum annual net income of energy stored in the partition as the objective function. Finally, the improved IEEE-33 bus distribution network is used to demonstrate the effectiveness and feasibility of the proposed model.

**INDEX TERMS** Energy storage system, sensitivity, partition, flame propagation model, location and capacity optimization, economic analysis.

## I. INTRODUCTION

In recent years, a large number of distributed sources (DG) have been connected to the distribution network, which has a certain impact on the traditional distribution network, and the safety and stability of the power system has been challenged. Wind and solar power output is random and uncertain [1], which is greatly affected by weather and geographical environment. When connected to the grid, the fluctuation of the output will bring a certain test to the security and stability of the grid and affect the power quality. Besides, due to a certain difference in the timing of the DG output and the load, during the peak period of the output, the DG cannot be completely absorbed and is forced to "abandon the wind", "abandon the solar". When the DG output is too large, problems such as node voltage threshold-crossing may occur. The distributed ESS has the characteristics of fast response speed, high power throughput ability and flexible location [2]. It has a good application prospect in improving the status of DG access [3]. However, due to the relatively high cost of energy storage investment [4], the energy storage allocation

is also not reasonable. Therefore, it is necessary to study the optimal allocation of distributed energy storage and explore the site-selection method under large-scale distributed energy storage deployment.

At present, a large number of scholars have researched the optimal configuration of energy storage. In general, distributed energy storage application scenarios mainly include the power supply side [5], the power grid side [6], [7] and the user side [8]. [8] developed economic investment strategies during the entire lifetime of energy storage based on the energy storage lifetime cost model. In [9], a method to evaluate the value of energy storage to support PV access is proposed. The total cost is the objective function. It is considered that under the existing investment cost, the energy storage itself is not economic. [10] established a two-layer optimization model of location and capacity, and proposed an intelligent algorithm to solve the model. In [11], the energy storage location and capacity optimization model was established with the system node voltage fluctuation, load fluctuation and total energy storage capacity as the target. An improved multi-objective particle swarm optimization algorithm is proposed to solve the model. In [12], [13], a storage energy optimization location algorithm based on

The associate editor coordinating the review of this manuscript and approving it for publication was Salvatore Favuzza<sup>1</sup>.

network loss sensitivity is proposed, and the node with the highest sensitivity coefficient is used as the energy storage grid-connected point. [14] proposed a heuristic optimization algorithm based on clustering and voltage sensitivity for site selection research.

The above literature has carried out a lot of work for the optimal location and capacity of large-scale distributed ESS to access to the grid-side and user-side. For location optimization, the current research is roughly divided into two ideas. The first is to establish a complex location selection model and solve the model through an intelligent algorithm, which is not very practical for a complex distribution network system. The second is to establish a site selection model based on voltage or network loss sensitivity. However, due to the linear representation of the power equation used in the sensitivity matrix, there is a certain error in only using the sensitivity coefficient as the location index. For the capacity optimization, existing methods generally consider the ESS capacity requirements from the perspective of power balance, ignoring the coupling relationship between the energy storage access location, service radius and the energy storage capacity: the larger the energy storage capacity, the larger the service radius and the investment; the smaller the energy storage capacity, the smaller the service radius, and the benefits in terms of improving power supply reliability will also decrease. At the same time, the energy storage layout and service radius are closely related to the voltage distribution and network loss of the grid. Few studies have considered the optimal allocation of energy storage from the perspective of comprehensively optimizing energy storage capacity and service radius to obtain higher economic benefits.

Given the shortcomings of current research, this paper proposes a more practical distributed ESS location selection model. First, establish a location selection model based on weighted voltage sensitivity. This model takes the voltage offset of the distribution network and the optimal loss of the active network as the objective function and uses the enumeration method to sequentially select the set of grid-connected nodes as the grid-connected points for power flow calculation, which greatly reduces the calculation amount. Then, establish an ESS capacity optimization method based on the flame propagation model. Based on the traditional flame propagation model, considering factors such as the distribution network grounding load type, network topology structure, and ESS power limit, introduce indexes such as node flammability, flame propagation wind direction, and flame propagation speed to coordinate and optimize the relationship between capacity, service radius, and economic benefits, and establish ESS partition method based on improved flame propagation model. Based on partition, a practical method for solving ESS power is presented. The method is simple and easy to implement and has engineering practicability. Under the premise of known the power of ESS, the power efficiency, reliability benefit, and electricity price benefit are comprehensively considered, and the energy storage capacity optimization model is established with the maximum annual

net income as the objective function. Finally, the feasibility and effectiveness of the proposed optimal configuration model are verified by the IEEE 33-node distribution network system.

This paper is organized as follows: In section II the weighted voltage sensitivity is established. In section III, the distributed energy storage site selection model is given. In section IV, the ESS capacity optimization model is established. In section V, the improved flame propagation model is introduced. In section VI, the site and capacity optimization process of ESS based on a partition is introduced. In section VII, case study results are presented to validate the proposed method, followed by the conclusions in section VIII.

## II. WEIGHTED VOLTAGE SENSITIVITY

### A. NODE VOLTAGE SENSITIVITY

When a node is connected to a PV system, the relationship between the change of node voltage and the amount of input power is derived as follows:

$$\begin{pmatrix} \Delta P \\ \Delta Q \end{pmatrix} = \begin{pmatrix} J_{P\delta} & J_{PU} \\ J_{Q\delta} & J_{QU} \end{pmatrix} \begin{pmatrix} \Delta\delta \\ \Delta U \end{pmatrix} = \begin{pmatrix} J_{P\delta}\Delta\delta + J_{PU}\Delta U \\ J_{Q\delta}\Delta\delta + J_{QU}\Delta U \end{pmatrix} \quad (1)$$

where  $\Delta P$  and  $\Delta Q$  are active change and reactive change.

$\Delta\delta$  and  $\Delta U$  are the voltage phase angle change and amplitude change.  $J_{P\delta}$ ,  $J_{PU}$ ,  $J_{Q\delta}$  and  $J_{QU}$  are the Jakabi Matrix Parameters. Assume  $\Delta Q = 0$ , we can obtain:

$$\Delta U = \frac{1}{(J_{PU} - J_{P\delta}J_{Q\delta}^{-1}J_{PU})} \Delta P = J \Delta P \quad (2)$$

where  $J$  is the Node Voltage - Active Sensitivity.

Depending on the formula (2), define the value of the  $\lambda_{ii}$  and the  $\lambda_{ij}$  as the node voltage-active sensitivity factor and the mutual sensitivity coefficient, respectively. Wherein, the  $\lambda_{ii}$  indicates that the node  $i$  injects power causes the change of node  $i$  voltage, and the  $\lambda_{ij}$  indicates that the node  $j$  injects power causes the change of node  $i$  voltage.

$$\begin{cases} \lambda_{ii} = \frac{\Delta U_i}{\Delta P_i} \\ \lambda_{ij} = \frac{\Delta U_i}{\Delta P_j} \end{cases} \quad (3)$$

When multiple nodes in the system inject power, the voltage sensitivity of node  $i$  should be the result of a combined interaction between self-sensitivity and interoperability, the functional relationship is as follows:

$$\lambda_i = f(\lambda_{ii}, \lambda_{ij}) \quad (4)$$

### B. WEIGHTED NODE VOLTAGE SENSITIVITY

Conventional voltage sensitivity can only measure the magnitude of the voltage change in the event of a power change in the node. However, from the perspective of net loss, energy storage and network outlets should try to select PV system grid-connected nodes. Depending on the formula (4),

although some nodes are not equipped with PVs, due to the impact of the power injection of adjacent nodes, the node voltage changes will be greater than the voltage changes of the node installed with PVs. Therefore, weighted node voltage sensitivity is constructed based on whether the node is equipped with a PV system, the functional relationship is:

$$Z_i = \omega \lambda_{i,t_0} \quad (5)$$

where  $Z_i$  is the weighted voltage sensitivity of node  $i$ ,  $\omega$  is the Weighted factor of node  $i$ , when node  $i$  is equipped with a PV system, its value is 1, and the opposite is 0.5.

### III. ESS SITE OPTIMIZATION MODEL

#### A. ALTERNATIVE GRID-CONNECTED NODES

According to the above method, for the node of  $Z_i > Z_0$ , it is regarded as the grid-connected node collection  $\Omega_c$  for store energy grid connection. Because the voltage sensitivity matrix is a linear representation of the power equation, there is a certain error between the result and the real value, so the grid-connected node collection  $\Omega_c$  obtained according to the weighted sensitivity method should be further analyzed to determine the final grid-connected node.

#### B. FINAL GRID-CONNECTED NODE

Based on the alternative grid-connected node, the final grid-connected node should be the node that minimizes the voltage deviation of the entire system after the energy storage system is installed, at the same time, the active power loss of the distribution network should be minimized. Therefore, this paper selects the node voltage deviation and network loss as the objective function, and use the enumeration method to solve it.

#### 1) OBJECTIVE FUNCTION

Node voltage deviation. Since the grid node identified by weighted sensitivity analysis is the node with the most voltage offset, it is necessary to weigh the voltage deviation of the grid-connected node and the voltage deviation of other nodes. Therefore, the sum of the voltage deviation of the grid-connected node selected by weight coefficient and the voltage deviation of other nodes is selected as the objective function, and the mathematical relationship is:

$$f_1 = \tau_1 \sum_{i \in \Omega_c} |U_i - U_N| + \tau_2 \sum_{j \in \Omega_o} |U_j - U_N| \quad (6)$$

where  $\tau_1$  and  $\tau_2$  are the weight factor, its value ranges from 0 to 1, and satisfy  $\tau_1 + \tau_2 = 1$ .  $\Omega_c$  is the web-side node collection,  $\Omega_o$  is the Other node collections.

System active network loss. Because the different access point of storage energy has a great impact on the distribution network active network loss, the size of the system network loss needs to be considered. The formula is:

$$f_2 = \sum_{l=1}^L P_{loss,l} \quad (7)$$

where  $P_{loss,l}$  is the active net loss of branch  $l$ ,  $L$  is the Total branch number in the distribution network.

Considering the node voltage deviation and the active power loss of the distribution network, the objective function of energy storage site selection is:

$$\min f = \xi_1 f_1 + \xi_2 f_2 \quad (8)$$

where  $\xi_1$  and  $\xi_2$  are the weight factor, its value ranges from 0 to 1, and satisfy  $\xi_1 + \xi_2 = 1$ .

#### 2) CONSTRAINTS

System power flow constraints can be primarily taken into account:

$$\begin{cases} P_{PV,t} + P_{grid,t} = P_{load,t} + P_{loss,t} + P_{ESS,t} \\ U_{min} \leq U_{i,t} \leq U_{max} \end{cases} \quad (9)$$

where  $P_{grid,t}$  and  $P_{loss,t}$  are the real-time power and line functional loss provided by the grid,  $U_{max}$  and  $U_{min}$  are the Upper and lower limits of node voltage.

### IV. ESS CAPACITY OPTIMIZATION MODEL

#### A. OBJECTIVE FUNCTION

This paper determines the capacity of the ESS to maximize the annual net benefits at the planning level which comprehensively considers the benefits and costs of ESS. In engineering practice, the power and capacity of ESS are usually integers, so the integer programming method is used to obtain the optimal power and capacity of ESS, and its objective function can be expressed as:

$$\max f(P_{ESS}, E_{ESS}) = f_1 + f_2 + f_3 - f_4 \quad (10)$$

where  $P_{ESS}$  is the optimized power,  $E_{ESS}$  is the optimized capacity,  $f_1$  is the annual electricity benefit brought of consuming RE,  $f_2$  is the annual reliability benefit of improving power supply reliability,  $f_3$  is the electricity benefit using time-of-use (TOU) electricity price and  $f_4$  is the annual equivalent cost of ESS.

Constraints include power constraints, capacity constraints, and SOC constraints:

$$0 \leq P_{ESS,c(t)} \leq P_{ESS} \quad (11)$$

$$0 \leq P_{ESS,d(t)} \leq P_{ESS} \quad (12)$$

$$E_{ESS,c} = \int_{t_{c1}}^{t_{c2}} P_{ESS,c(t)} dt \leq E_{ESS} \quad (13)$$

$$E_{ESS,d} = \int_{t_{d1}}^{t_{d2}} P_{ESS,d(t)} dt \leq E_{ESS} \quad (14)$$

$$E_{ESS,c} = E_{ESS,d} \quad (15)$$

$$0.1 \leq SOC \leq 0.9 \quad (16)$$

where  $P_{ESS,c(t)}$  and  $P_{ESS,d(t)}$  are the charge and discharge power of ESS, respectively.  $E_{ESS,c}$ , and  $E_{ESS,d}$  are the charge and discharge capacity of ESS, respectively.  $t_{c1}$  and  $t_{c2}$  correspond to the start and end time of charging, respectively.  $t_{d1}$  and  $t_{d2}$  correspond to the start and end time of discharging, respectively. SOC is the state of charge of ESS.

## B. BENEFITS ANALYSIS OF ESS

### 1) ANNUAL ELECTRICITY QUANTITY BENEFIT

Annual electricity benefit refers to the benefit of reducing wasted solar-power generation capacity after the configuration of ESS [18], [19]. Mathematically, this can be described as:

$$f_1 = \sum_{i=1}^{365} \beta_{RE} E_{RE} \quad (17)$$

where  $\beta_{RE}$  is the generation price of PV,  $E_{RE}$  is the annual amount of PV capacity to be adopted during planning years.

$$E_{RE} = \int_{t_a}^{t_b} P_{CD}(t) dt \quad (18)$$

$$P_{CD}(t) = \begin{cases} P_{YX}(t) & P_{YX}(t) \leq P_{ESS} \\ P_{ESS} & P_{YX}(t) > P_{ESS} \end{cases} \quad (19)$$

where  $t_a$  and  $t_b$  are the starting and ending time for PV to exceed the limit, respectively,  $P_{CD}(t)$  is the charging power of ESS consuming PV, and  $P_{YX}(t)$  is the off-limits power of PV. According to the time sequence relationship between PV output and load output, the out-of-limit power of PV in the partition can be solved.

### 2) ANNUAL RELIABILITY BENEFIT

The reliability benefit is to reduce the economic loss caused by power outage due to faults such as lines and transformers after energy storage is configured. The calculation is:

$$f_2 = \sum_{n \in N} \sum_{m \in M_n} \overline{L}_m R_n \gamma (1 - \frac{T_S}{24}) \quad (20)$$

$$p = \begin{cases} 1 & T_S \geq T_\gamma \\ \frac{T_S}{T_\gamma} & T_S < T_\gamma \end{cases} \quad (21)$$

where  $M_n$  is the total number of nodes with load type  $n$ ,  $\overline{L}_m$  is the average load of node  $m$  during the power outage phase,  $\gamma$  is the average annual failure rate of distribution power station (times/a),  $R_n(T_\gamma)$  is The load type  $n$  due to the economic loss caused by the failure, this parameter is related to the time of power failure,  $p$  is the probability that the energy storage service time is greater than the failure time,  $T_\gamma$  is the failure time,  $T_S$  is the energy storage discharge time.

### 3) ANNUAL ELECTRICITY PRICE BENEFIT

When the configured ESS capacity is larger than the off-limit PV capacity, the excess capacity will generate electricity price benefit. The price benefits refers to the arbitrage of using TOU price, in which the ESS can charge when the price is low and discharge when the price is high. Mathematically, this can be described as:

$$f_3 = \sum_{i=1}^{365} (e_p - e_v)(E_{ESS} - E_{RE}) \quad (22)$$

where  $e_p$  and  $e_v$  are peak and valley price, respectively.

## C. ANNUAL COST

The costs of ESS include equipment investment in the initial stage and operation and maintenance cost in the later stage. Annual equivalent cost is related to equipment investment, operation and maintenance cost, lifetime and capital discount rate [20]. Mathematically, this can be described as follows:

$$f_4 = (\lambda_P P_{ESS} + \lambda_E E_{ESS}) \frac{r(1+r)^{Y_{ESS}}}{(1+r)^{Y_{ESS}} - 1} + \lambda_{O\&M} P_{ESS} \quad (23)$$

where  $\lambda_P$  is the cost of unit power of ESS(¥/kW),  $\lambda_E$  is the cost of the unit capacity of ESS(¥/kW•h),  $\lambda_{O\&M}$  is the annual operating and maintenance costs of unit power of ESS,  $r$  is the capital discount rate, and  $Y_{ESS}$  is the life span of ESS.

## V. IMPROVED FLAME PROPAGATION MODEL

### A. FLAME PROPAGATION MODEL

Once the flame is ignited, it will spread around in the combustible medium. Assuming that the combustible medium around is uniform, the flame will spread uniformly around until it encounters non-combustible substance (boundary) or adjacent flame. After the combustible medium is exhausted, the flame goes out, and the ashes produced by flame combustion is the range of flame propagation.

Assuming a set of central points  $\Omega = \{\Omega_1, \Omega_2, \dots, \Omega_n\}$ ,  $3 \leq n \leq N$ , then the flame propagation region of arbitrary points can be represented as follows:

$$V(\Omega_i) = \bigcap_{1 \leq j \leq N, j \neq i} \{x | d(x, \Omega_i) \leq d(x, \Omega_j)\} \quad (i = 1, 2, \dots, n) \quad (24)$$

where  $V(\Omega_i)$  is the spread range of flame center for  $\Omega_i$ ,  $d(x, \Omega_i)$  is the euclidean distance between the point  $x$  and flame center  $\Omega_i$ , and  $x$  is the point on the plane.

The partition idea has many practical applications in the power system, such as substation power supply partition [19], micro-grid partition, etc. Based on this, an energy storage partition method based on the flame propagation model is established. The division of the ESS service area can draw on the flame propagation model, with the ESS access point as the center of the flame, spreading in all directions along the road. The ash generated by flame combustion is the ESS service area, the time that the flame burns is the length of the energy storage service.

### B. THE FLAMMABILITY INDEX OF BUS

This paper mainly considers the role of ESS connected to the distribution network in consuming PV output power and improving the reliability of power supply. Therefore, PV and important load buses should be prioritized in the ESS service area. The flammability index of nodes  $s_i$  is defined as the product of node power and the membership degree  $\lambda_n$  to quantitatively evaluate the priority of the bus in the ESS service area. Mathematically, this can be described



as follows:

$$\begin{cases} s_i = \sum_{n \in N} \lambda_n P_{i,n} \\ \lambda_n = \frac{\Delta g_n - \Delta c}{\Delta c} \end{cases} \quad (25)$$

where  $\Delta c$  is the unit investment of ESS,  $\Delta g_n$  is the unit benefit generated by type  $n$  power node. Power types include PV, residential, commercial, and industrial loads. The power of a node may have multiple types, for example, there are both PV system and important loads, so the flammability of the node is the sum of the product of different types of power and the corresponding revenue membership.  $P_{i,n}$  is the power of type  $n$  in node  $i$ .

When  $\lambda_n$  exceeds 5%, it has an economic benefit to divide node  $i$  into the ESS supply area. Otherwise, it has no benefit. To maximize the economic benefits of ESS, the threshold value  $s_0$  of  $s_i$  can be set according to the actual grid data. When  $s_i$  is lower than  $s_0$ , it is generally considered that the node is not combustible. When  $s_i$  is higher than  $s_0$ , the node is considered combustible, and these nodes are taken as alternative nodes of energy storage partition.

### C. THE DIRECTION OF FLAME

The division of ESS service area should not only ensure the load power supply and consuming PV energy as much as possible, but also facilitate the operation and management of the distribution network. Therefore, in the process of flame propagation, factors such as the location and topological structure of the bus in the distribution network are taken into account. The concepts of downwind and upwind of flame propagation are introduced to describe the network topology. Downwind means that ESS and load nodes are on the same branch or line along the current trend direction. The upwind means the opposite direction of the power flow or ESS and load nodes are in different branches or lines. Therefore, the wind direction  $f_i$  is introduced to comprehensively evaluate the priority of the bus. Mathematically, this can be described as follows:

$$f_i = (\delta_1 s_i + \delta_2 p_i) c_i \quad (26)$$

where  $\delta_1$  and  $\delta_2$  are weighting factors,  $p_i$  is the topological coefficient =  $m_i/n_i$ ,  $m_i$  is the branch number of the bus  $i$ ,  $n_i$  is the layer number of the bus  $i$ . A larger  $p_i$  indicates that the node has more branches, fewer layers, more energy storage power supply load, and a smaller service radius, and this node should be preferentially assigned to the energy storage service area.  $c_i$  is the coefficient of node tidal direction. When node  $i$  is in the downstream direction of the flame,  $c_i$  equals 1. Otherwise,  $c_i$  equals 0.5.

IEEE 13 bus distribution network is taken as an example to illustrate the practical significance of the above parameters. As shown in figure 1, it is assumed that the access point of ESS is node 3. Comparing with node 4, node 2 has more branches than node 4, and node 2 has fewer layers than node 4, so  $p_2 > p_4$ . Node 2 is in the upwind position,

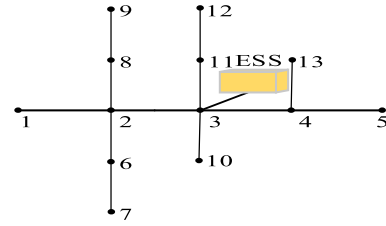


FIGURE 1. IEEE 13 bus distribution network structure.

and node 4 is in the downwind position, so  $c_2=0.5$ ,  $c_4=1$ . On the premise that the flammability indexes of node 2 and node 4 are known, then, the wind direction of the two nodes can be judged and the priority of the two nodes can be finally determined.

### D. THE PROPAGATION SPEED OF FLAME

The propagation speed of flame is constant in the conventional flame propagation model. In fact, as the service radius of ESS increases, the load rate of ESS increases, then propagation speed will decrease. According to the current load rate of ESS and power supply radius, the flame propagation speed  $v_i$  is constructed. Mathematically, this can be expressed as:

$$v_i = \alpha_1(1 - l_i) + \alpha_2 r_i \quad (27)$$

$$l_i = \frac{\sum_{j \in \Omega} P_j + P_i}{P_U} \quad (28)$$

$$r_i = \frac{D_o - D_i}{D_o} \quad (29)$$

where  $l_i$  is the load rate of ESS after the bus  $i$  belongs to the service area,  $r_i$  is the service radius of ESS,  $\alpha_1$  and  $\alpha_2$  are weighting factors,  $P_U$  is the upper limit power of ESS in partition,  $P_i$  is the power of bus  $i$ , and  $P_j$  is the total power of the buses which belong to the service area.  $D_0$  is the reference value of the service radius, which is related to the upper limit of the energy storage power. The larger the energy storage power, the larger the service radius.  $D_i$  is the actual distance from bus  $i$  to the access point of ESS.

### E. ADJUSTMENT OF FLAME DIFFUSION DIRECTION

During the flame diffusion process, if the service radius in a certain direction exceeds the reference value, the diffusion in this direction ends. The flame needs to adjust its direction of diffusion until the end of the diffusion in all directions.

Also, the adjacent flames will meet during flame diffusion. As shown in figure 2, the dashed arrows indicate the

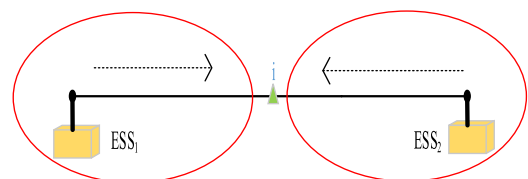


FIGURE 2. The meeting of adjacent flames.

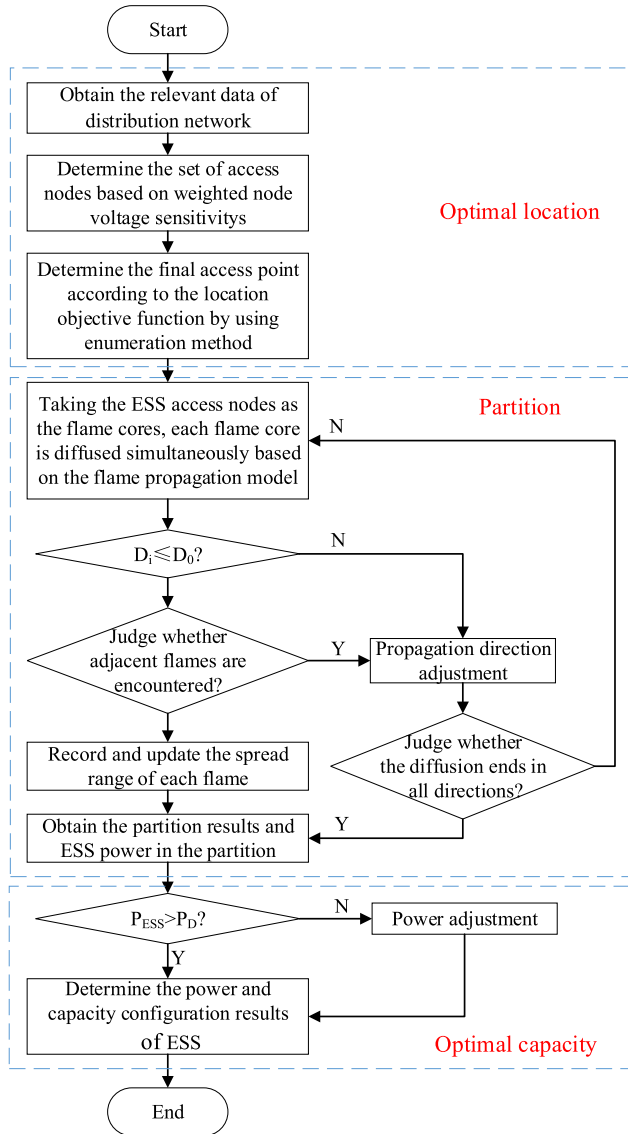


FIGURE 3. Capacity optimization process.

direction of flame diffusion. In this case, it is only necessary to determine the attribution problem of the boundary node while adjusting the diffusion direction of the two flames. Two ESS access points are used as flame cores respectively. The boundary node belongs to the ESS service area with a large product by calculating  $(f_i v_i)_1$  and  $(f_i v_i)_2$ .

### F. ESS POWER AND CAPACITY DETERMINATION

According to the node flammability index, the alternative nodes have economic value and high return on investment. Therefore, the energy storage access power in the sub-region is the sum of the load power of the alternative node in the sub-region and the maximum amount of the over-limit power of the PV in the sub-region, which can be expressed as:

$$P_{ESS,n} = \max\left\{ \sum_{i \in \Omega_n} P_{YXi}(t), \sum_{i \in \Omega_n} P_{Li}(t) \right\} \quad (30)$$

where  $P_{ESS,n}$  is the configured power of ESS in partition  $n$ .

After determining the ESS power in each partition, the integer programming method is used to solve the ESS capacity  $E_{ESS,n}$  in each partition, according to the ESS capacity optimization model mentioned above.

## VI. THE PROCESS OF SITE AND CAPACITY SELECTION FOR DISTRIBUTED ENERGY STORAGE

This paper mainly includes ESS site optimization and capacity optimization. The specific steps are as follows:

*Step1:* Obtain the relevant data of the distribution network, including distribution network topology, node load size, and type, PV systems installed capacity and access points.

*Step2:* The set of energy storage grid-connected nodes is determined according to the weighted node voltage sensitivity.

*Step3:* Use the enumeration method to calculate power flow again with each node in the grid-connected node-set as the energy storage grid-connected point. Calculate the objective function to determine the grid connection point for the final energy storage.

*Step4:* With the energy storage access point as the flame center, the diffusion is performed based on the improved flame propagation model. The flame diffusion direction is determined according to the node flammability index, the node topological characteristic coefficient, and the node power flow direction coefficient. The flame diffusion speed is determined based on the energy storage load factor and service radius factor.

*Step5:* Determine whether the radius constraint is satisfied during each flame diffusion process. If the radius constraint is not met, the flame needs to adjust the direction of diffusion.

*Step6:* Determine whether adjacent flames are encountered during flame diffusion. If the adjacent flame is encountered, the diffusion direction needs to be adjusted. The adjustment of flame diffusion direction is introduced in the following text. After the direction of diffusion is adjusted, judge whether the flame is diffused in all directions. If the diffusion ends, the flame stops diffusing and the partition result is obtained. If not, go back to step 2 and continue to spread.

*Step7:* Record and update the range of flame diffusion.

*Step8:* When all the flame propagation is over, the final ESS partition results are obtained, and the ESS optimized power in the partition is determined.

*Step9:* Determine whether the optimized power in the partition meets the constraint. If the upper and lower power constraints are not met, the optimized power in the partition needs to be adjusted. Otherwise, go to the next step.

*Step10:* The ESS power and capacity configuration results are determined based on the final partition results.

## VII. CASE STUDY

### A. THE DATA OF EXAMPLES

IEEE 33 bus distribution network is used as an example, and the distance between nodes is set to 0.2km. The total load is 3715kW+j2300kvar. The load power of each node is shown in table 1. For the convenience of analysis,

TABLE 1. Active power of IEEE 33 nodes distribution network.

Node	Load/kW	Node	Load/kW	Node	Load/kW
0	/	11	60	22	90
1	100	12	60	23	420
2	90	13	120	24	420
3	120	14	60	25	60
4	60	15	60	26	60
5	60	16	60	27	60
6	200	17	90	28	120
7	200	18	90	29	200
8	60	19	90	30	150
9	60	20	90	31	210
10	45	21	90	32	60

the industrial load is defined as the power over 400kW, the commercial load is defined as the power between 100kW and 400kW, and the residential load is defined as the power below 100kW. In nodes 17, 22, 24, 31 and 32, respectively, access 1.8MW, 0.3MW, 1.2MW, 0.2MW and 1.0MW of distributed PV systems. The system’s rated voltage is 12.66kV, the single ESS access power lower limit  $P_D$  is 400kW, and the power upper limit  $P_U$  is 6000kW [21]. The load peak price period is from 8:00 to 22:00, and the valley price period is from 22:00 to 8:00.

Since the load curve corresponding to different types of loads has different trends, this paper considers the load and the timing of PV output. The curves of residential load, industrial load, commercial load, and PV output are all using the typical daily curves provided by Homer software developed by the National Renewable Energy Laboratory (NREL). The typical daily curve is shown in figure 4.

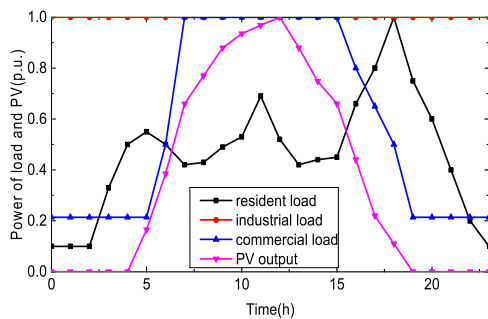


FIGURE 4. Typical daily curve.

TABLE 2. Outage cost functions of all kinds of customer ( ¥ /kW).

Duration	20min	1h	4h	8h
residential load	0.465	2.4	24.57	78.45
commercial load	14.85	42.76	156.86	415.04
industrial load	19.34	45.43	125.82	279.04

Table 2 shows the loss due to power out of various load [22]. Table 3 gives the system parameters required for the example [23]–[25].

TABLE 3. System parameters.

Parameters	Values	Parameters	Values
$r$	0.05	$s_0$	5
$\beta_{RE}(\text{¥/kW}\cdot\text{h})$	1.12	$Y_{ESS}(\text{a})$	10
$\lambda_P(\text{¥/kW})$	1000	$T_r(\text{h})$	5
$\lambda_E(\text{¥/kW}\cdot\text{h})$	1880	$\gamma(\text{f/a})$	0.34
$\lambda_{O\&M}(\text{¥/kW})$	24	$e_p(\text{¥/kW}\cdot\text{h})$	0.88
$D_0(\text{km})$	1.2	$e_v(\text{¥/kW}\cdot\text{h})$	0.28
$\tau_1/\tau_2$	0.2/0.8	$\xi_1/\xi_2$	0.4/0.6

TABLE 4. Voltage, sensitivity and weighted sensitivity parameters.

Node	Voltage/pu	$\lambda_i$	$Z_i$
0	1	0	0
1	1.000	0.003	0.002
2	0.999	0.016	0.008
3	0.999	0.024	0.012
4	0.999	0.031	0.015
5	0.996	0.046	0.023
6	0.994	0.048	0.024
7	0.997	0.056	0.028
8	1.002	0.067	0.033
9	1.007	0.078	0.039
10	1.009	0.081	0.040
11	1.011	0.084	0.042
12	1.021	0.100	0.050
13	1.024	0.105	0.052
14	1.029	0.112	0.056
15	1.036	0.120	0.060
16	1.048	0.134	0.067
17	1.055	0.142	0.142
18	0.999	0.002	0.001
19	0.996	0.003	0.001
20	0.995	0.003	0.001
21	0.994	0.002	0.001
22	1.002	0.023	0.023
23	1.004	0.031	0.031
24	1.014	0.045	0.045
25	0.995	0.047	0.023
26	0.995	0.050	0.025
27	0.992	0.058	0.029
28	0.991	0.065	0.032
29	0.991	0.069	0.034
30	0.995	0.077	0.038
31	0.996	0.079	0.079
32	0.998	0.081	0.081

B. ENERGY STORAGE SITE SELECTION RESULTS

The IEEE33 node system is built in MATLAB, and the power flow calculation is carried out according to the case study. The voltage, general sensitivity and weighted sensitivity parameters of each node after being connected to the PV system are shown in table 4.

Assume  $Z_0 = 0.045$ , for the node of  $Z_i > Z_0$ , it is regarded as the grid-connected node, so the ESS grid-connected alternate nodes are set up as {12, 13, 14, 15, 16, 17, 24, 31, 32}. These nine nodes are used as ESS grid-connected points for power flow calculation. The results of the target function calculation are shown in table 5.

As can be seen from table 5, node 17 is the best grid-connected node for ESS. Figure 5 shows the original

TABLE 5. Alternative node target function calculation value.

Node	$f_1$	$f_2$	$f$
12	0.400	0.149	0.249
13	0.405	0.142	0.247
14	0.417	0.133	0.246
15	0.421	0.122	0.241
16	0.422	0.099	0.228
17	0.414	0.086	0.217
24	0.303	0.186	0.233
31	0.454	0.190	0.296
32	0.452	0.187	0.293

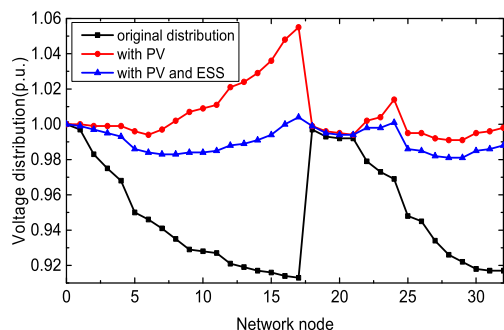


FIGURE 5. Voltage distribution of IEEE33 node distribution.

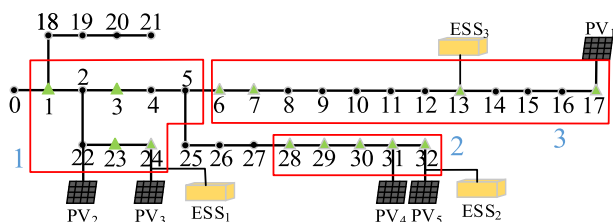


FIGURE 6. Initial partition results.

voltage distribution, the voltage distribution with DG, and the voltage distribution after node 17 is connected to the ESS of IEEE33 node distribution network.

As can be seen from figure 5, distributed ESS access can effectively suppress the problem of voltage limit and make the voltage deviation of the whole system smaller.

C. ENERGY STORAGE CAPACITY OPTIMIZATION RESULTS

Select nodes 13, 24 and 32 as ESS grid-connected points, the energy storage partition results are obtained according to the improved flame propagation model. As shown in figure 6, the triangle in the figure represents the alternative node in a partition.

According to the partition results, the alternative node load power and PV overpass power are obtained in each partition, and the ESS access power in the partition can be calculated according to the formula (30), the specific data are shown in table 6.

From table 6, we know that ESS access power meets the power upper and lower limit constraints.

Based on the results of partition, according to the energy storage capacity optimization model, the ESS capacity in

TABLE 6. ESS access power of each partition.

Partition	$P_{ESS,n}/kW$	Whether the power constraint is satisfied
1	440	Yes
2	680	Yes
3	1280	Yes

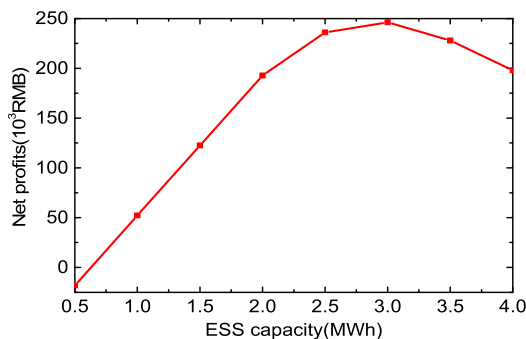


FIGURE 7. Capacity optimization results in partition 1.

TABLE 7. Comparison of active power network losses.

Scenery	Install node/ power (kW)	Active network loss/kW·h
without ESS	\	202
centralized ESS	0/2400	79
distributed ESS	13/1280,24/440,	48
partition	32/680	

each partition is solved by the integer planning method. Since each partition is calculated similarly, partition 1 is used as an example. The discharge depth of the ESS is 80%, and the relationship between net profits and ESS capacity is shown in figure 7.

From figure 7, it can be known that when the power is constant, as the ESS capacity increases, the net income increases first and then decreases. And when the 440kW/ 2840 kW•h ESS is configured in the partition, the maximum net profits are 236,500 RMB.

Similarly, when the partition 2 is equipped with an ESS of 680 kW/4020 kW•h, the net profits reach a maximum of 268,800 RMB. When the partition 3 is equipped with an ESS of 1280 kW/7130 kW•h, the net profits reach a maximum of 322,500 RMB. In summary, a total of 2400kW/13900 kW•h distributed ESSs are required for the distribution network.

The following will explain the advantages of configuring distributed ESS and partition planning from indicators such as active power network loss, annual investment and net profits, PV consumption ability and load outage loss.

Table 7 shows the comparison of active network losses in the three scenarios of IEEE33 node distribution network system: without ESS, centralized ESS, and distributed ESS.



**TABLE 8. Comparison of annual investment and net profits.**

Planning method	Investment /10 <sup>3</sup> ¥	Net profits /10 <sup>3</sup> ¥	Annual rate of profits (%)
conventional planning	3418.7	687.2	20.1
partition planning	3688.4	827.8	22.4

**TABLE 9. Comparison of PV consumption ability and load outage loss.**

Optimization indicator	PV Consumption ability	Load outage loss(10 <sup>3</sup> ¥)/a
before access	76.5%	172.6
after access	100%	42.8

It can be known from table 7 that the configuration of distributed ESS can reduce the active power loss of the system. Compared with the centralized ESS, the distributed ESS partition planning can effectively reduce the active power loss of the system.

Current energy storage planning methods generally configure distributed ESS from the perspective of power shortages, and a specific method will not be described in detail. According to this method, a total of 1980kW/12935 kWh distributed ESSs are required to consume renewable energy. Table 8 shows the comparison of the annual investment cost and annual net income calculated by the two scenarios: ESS partition planning and conventional planning.

As can be seen from table 8, compared with the conventional planning method, although partition planning generally requires larger ESS capacity, the net profits and annual rate of profits have been improved, so it has better economic benefits.

Table 9 gives a comparison of PV consumption ability and load outage loss before and after the ESS configured.

It can be seen from table 9 that after energy storage configured, PV consumption capacity in the partition has been improved. Also, the loss of load power outages also decreased more.

## VIII. CONCLUSION

In this paper, given the current situation of large-scale ESS access in the distribution network, a practical distributed ESS location and capacity optimal model is proposed, and the following conclusions are drawn.

1) The capacity optimization method based on the partition can reduce the system's active network loss, and can improve the PV consumption ability and improve the power supply reliability of the distribution network. The ESS partition weights the contradiction between the scope of service and the benefits to some extent.

2) Distributed ESS access can play a supporting role in the entire distribution network voltage, and has a good regulatory effect in the large-scale DG grid-connected scene.

3) The proposed distributed ESS location optimization method, which is improved based on the original voltage sensitivity, not only greatly reduces the calculation but also makes up for the deficiency of the sensitivity coefficient as the location index.

## REFERENCES

- [1] V. F. Martins and C. L. T. Borges, "Active distribution network integrated planning incorporating distributed generation and load response uncertainties," *IEEE Trans. Power Syst.*, vol. 26, no. 4, pp. 2164–2172, Nov. 2011.
- [2] Z. Qiao and J. Yang, "Comparison of centralised and distributed battery energy storage systems in LV distribution networks on operational optimisation and financial benefits," *J. Eng.*, vol. 2017, no. 13, pp. 1671–1675, Jan. 2017.
- [3] G. D. Xu and H. Z. Cheng, "Optimal placement and sizing of distributed generator units using genetic optimization algorithm," *Electr. Power Compon. Syst.*, vol. 46, no. 3, pp. 342–352, 2018.
- [4] S. Sabihuddin, A. Kiprakis, and M. Mueller, "A numerical and graphical review of energy storage technologies," *Energies*, vol. 8, no. 1, pp. 172–216, Dec. 2014.
- [5] C. Parker, "Lead-acid battery energy-storage systems for electricity supply networks," *J. Power Sources*, vol. 100, nos. 1–2, pp. 18–28, Nov. 2001.
- [6] H. Mehrjerdi, "Simultaneous load leveling and voltage profile improvement in distribution networks by optimal battery storage planning," *Energy*, vol. 181, pp. 916–926, Aug. 2019.
- [7] M. Nick, M. Hohmann, R. Cherkaoui, and M. Paolone, "Optimal location and sizing of distributed storage systems in active distribution networks," in *Proc. IEEE Grenoble Conf.*, Grenoble, France, Jun. 2013, pp. 232–240.
- [8] J. H. Xue and J. L. Ye, "Economic feasibility of user-side battery energy storage based on whole-life-cycle cost model," *Power Syst. Technol.*, vol. 40, no. 8, pp. 2471–2476, 2016.
- [9] Z. M. Yan and C. M. Wang, "Capacity plan of battery energy storage system in user side considering power outage cost," *Autom. Electr. Power Syst.*, vol. 36, no. 11, pp. 50–54, 2012.
- [10] Z. M. Yan and C. M. Wang, "Value assessment model of battery energy storage system in distribution network," *Electr. Power Autom. Equip.*, vol. 33, no. 2, pp. 57–61, 2013.
- [11] T. Fei and A. Marko, "Business case for distributed energy storage," in *Proc. Int. Conf. Exhib. Electr. Distrib.*, Glasgow, U.K., Jun. 2017, pp. 1605–1608.
- [12] J. H. Li and S. M. Wang, "Optimal combined peak-shaving scheme using energy storage for auxiliary considering both technology and economy," *Autom. Electr. Power Syst.*, vol. 41, no. 9, pp. 44–50, 2017.
- [13] C. H. Antunes, D. F. Pires, C. Barrico, Á. Gomes, and A. G. Martins, "A multi-objective evolutionary algorithm for reactive power compensation in distribution networks," *Appl. Energy*, vol. 86, nos. 7–8, pp. 977–984, Jul. 2009.
- [14] Y. Wang and Z. Cai, "Combining multiobjective optimization with differential evolution to solve constrained optimization problems," *IEEE Trans. Evol. Comput.*, vol. 16, no. 1, pp. 117–134, Feb. 2012.
- [15] S. Chakraborty, T. Funabashi, A. Saber, H. Toyama, and T. Senjyu, "Determination methodology for optimising the energy storage size for power system," *IET Gener., Transmiss. Distrib.*, vol. 3, no. 11, pp. 987–999, Nov. 2009.
- [16] Y. Zhang and B. Xiao, "A capacity configuration method for energy storage based on feasible operation region of wind power and life attenuation," *Electr. Power Construct.*, vol. 39, no. 4, pp. 60–66, 2018.
- [17] H. Temraz and M. Salama, "A planning model for siting, sizing and timing of distribution substations and defining the associated service area," *Electr. Power Syst. Res.*, vol. 62, no. 2, pp. 145–151, Jun. 2002.
- [18] S. A. Arefifar, Y. A.-R.-I. Mohamed, and T. H. M. El-Fouly, "Optimum microgrid design for enhancing reliability and supply-security," *IEEE Trans. Smart Grid*, vol. 4, no. 3, pp. 1567–1575, Sep. 2013.
- [19] P. M. Herder and A. N. Ajah, "Integration of societal outage cost into infrastructure design and maintenance optimization," in *Proc. IEEE Int. Conf. Syst., Man Cybern.*, San Antonio, TX, USA, Oct. 2009, pp. 265–271.
- [20] H. Mehrjerdi and R. Hemmati, "Electric vehicle charging station with multi-level charging infrastructure and hybrid solar-battery-diesel generation incorporating comfort of drivers," *J. Energy Storage*, vol. 26, Dec. 2019, Art. no. 100924.

- [21] *Design Code for Distributed Energy Storage Connecting to Distribution Network*, China Energy Standard T/CEC 173-2018, 2018.
- [22] F. Gao and K. Yang, "Cycle-life energy analysis of LifePO<sub>4</sub> batteries for energy storage," *Proc. CSEE*, vol. 33, no. 5, pp. 41–45, 2013.
- [23] G. Q. Wan and Z. Ren, "Calculation of customer's outage cost considering feeder automation," *Power Syst. Technol.*, vol. 29, no. 1, pp. 24–29, 2005.
- [24] X. Q. Xiu and W. Tang, "Comprehensive evaluation technology of energy storage configuration based on analytic hierarchy process," *Autom. Electr. Power Syst.*, vol. 42, no. 11, pp. 72–82, 2018.
- [25] M. Wu and X. J. Ren, "Optimal allocation method for capacity of power supply system in industrial park under new electricity market reform," *Autom. Electr. Power Syst.*, vol. 42, no. 5, pp. 2–8, 2018.



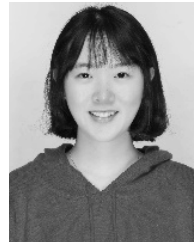
**XIAOBO TANG** received the B.S. degree in electrical engineering from the Harbin Institute of Technology, Harbin, China, in 1999, and the M.S. and Ph.D. degrees in power system and its automation from Southeast University, Nanjing, China, in 2005 and 2010, respectively. He is currently a Lecturer with the School of Electrical and Automation Engineering, Nanjing Normal University, Nanjing. His research interests include power grid planning, and distributed energy storage planning and control.



**KAI DENG** received the B.S. degree in electrical engineering from Anhui Jianzhu University, Hefei, China, in 2017. He is currently pursuing the M.S. degree in electrical engineering from Nanjing Normal University, Nanjing, China. His research interests include distribution network planning and energy storage optimization planning.



**QIUWEI WU** (Senior Member, IEEE) received the Ph.D. degree in power system engineering from Nanyang Technological University, Singapore, in 2009. He is currently an Associate Professor with the Department of Electrical Engineering, Technical University of Denmark (DTU). His research interests are operation and control of power systems with high penetration of renewables, including wind power modeling and control, active distribution networks, and operation of integrated energy systems.



**YULONG FENG** received the B.S. degree from the Anhui Institute of Information Technology, Wuhu, China, in 2018. She is currently pursuing the M.S. degree in electrical engineering from Nanjing Normal University, Nanjing, China. Her research interests include energy storage planning and operation control.

...